Evidence for a Target-Material Dependence of the Neutron-Proton Branching Ratio in d+d Reactions for Deuteron Energies below 20 keV

A. Huke, K. Czerski, T. Dorsch and P. Heide

Institut für Atomare Physik und Fachdidaktik, Technische Universität Berlin,
Hardenbergstr. 36, D-10623 Berlin, Germany

Angular distributions and the neutron-proton branching ratio of the mirror reactions ^{2}H(d,p)^{3}H and ^{2}H(d,n)^{3}He have been investigated using different deuterized metallic targets at projectile energies ranging from 5 to 60 keV. Whereas the experimental results obtained for Al, Zr, Pd and Ta targets do not differ from those known from gas-target experiments, an enhancement of the angular anisotropy in the neutron channel and a quenching of the neutron-proton branching ratio have been observed for Li and Sr targets at deuteron energies below 20 keV . Both effects can be explained assuming an induced adiabatic polarization of the reacting deuterons in the crystal lattice.

1 Introduction

As known for a long time from accelerator experiments the d+d fusion reactions have 3 possible outgoing channels, ^{2}H(d,p)^{3}H, ^{2}H(d,n)^{3}He and ^{2}H(d,γ)^{4}He. Two of them mediated by the strong interaction generate high energetic particles with a branching ratio of about 1 below 50 keV while the third one is an electromagnetic transition suppressed by $< 10^{-4}$. Close to the reaction threshold there are two 1^- resonances in the compound nucleus ^{4}He. They can be excited by deuterons with an orbital angular momentum of 1. This is the reason for the unusually strong anisotropy of the angular distribution of the ejectiles even at the lowest energies.

In our previous works [1, 2] we have found a strongly enhanced electron screening effect for the d+d reactions in metallic environments. Angular distributions and relative intensities of the proton and neutron channels investigated for d+d reactions taking place in Al, Zr, Pd and Ta targets were, however, in agreement with the results of gas-target experiments. Here we present

new results obtained for Sr, Li and Na targets giving a first evidence for an alteration of the neutron-proton branching ratio and the angular distributions. Initial results were presented in [3] and hitherto completely published in [4] but now a first theoretical explanation for this surprising observation can be presented [5].

2 Experimental results

The experiment has been carried out at a cascade accelerator optimized for low energy beams. The targets were pure metal disks becoming self-implanted deuterium targets under the deuteron irradiation. Four Si-detectors at the laboratory angles of 90°, 110°, 130° and 150° were used for the detection of all charged particles, p, t, ^{3}He, of the reactions ^{2}H(d,p)t and ^{2}H(d,n)^{3}He [6, 2]. The detectors needed to be shielded from the backscattered deuterons in order to prevent a congestion of them and the data acquisition system. Therefore grounded Al-foils of thicknesses from $120 - 150\,\mu g/cm^2$ were placed in front of the detectors insulated from them. The thickness is sufficient in order to stop backscattered deuterons up to 60 keV. The low energy part of some representative spectra from the 90°-detector is depicted in fig. 1 magnifying the two lines of the recoil nuclei ^{3}He and t. The spectra are normalized to an integral value of one in order to make them commensurable. The energies above the peaks are the kinetic energies of the ejectiles in the laboratory system. They drop for increasing projectile energies, which is especially significant for the back angle positions. The gray filled spectra are from Ta targets while the black and gray step lines are for Sr and Li and Na respectively. The two plots compare the form of the spectral lines at a low projectile energy of 8 keV to a high energy of 30 keV. At 8 keV the t-line of Ta is well separated while the ^{3}He-line sits on an exponential background. The background is subtracted by fitting an exponential function to the lowest energy part and then by extrapolating it to the high energies. The spectral lines for Sr are already broader with an enhanced low energy tail leading to an overlap of both lines. This effect becomes even stronger for Li and Na. At 30 keV the Ta lines are broader but the tails of the Sr, Li and Na lines are much more distinctive. The overlap of the two lines is even higher. For Li and Na the ^{3}He-line is hardly more than an edge. The p-line at 3 MeV has also a long low energy tail but it vanishes before the t-line. The appearence and the properties of these tails can be explained by a phenomenon known from the physical chemistry of the metal hydrides, called *embrittlement* [7] which means that the crystal structure of the metal is bursted by the recrystallization process that accompanies the formation of the metal hydride crystal. Reactive metals change their crystal structure while forming the metal hydride. If the hydration precedes not in a thermal equilibrium and relatively slow, the material cannot compensate the tension of the recrystallization process and bursts. Since deuteron implantation is far off the thermal equilibrium, embrittlement is a hardly avoidable concomitant phenomenon for reactive metals. How embrittlement effectuates the tails is elucidated with the sketch in fig. 1. Assuming, the projectile travels through the target along a path covering many empty regions, the energy loss becomes smaller and consequently the nuclear reactions occur deeper below the target surface than in the case of compact materials. Therefore the ejectiles that in turn can travel through more compact target regions loose more energy additionally contributing to the low energy tail of the particle spectrum. The increase of the tail with the projectile energy arises from the simultaneous increase in the overall range

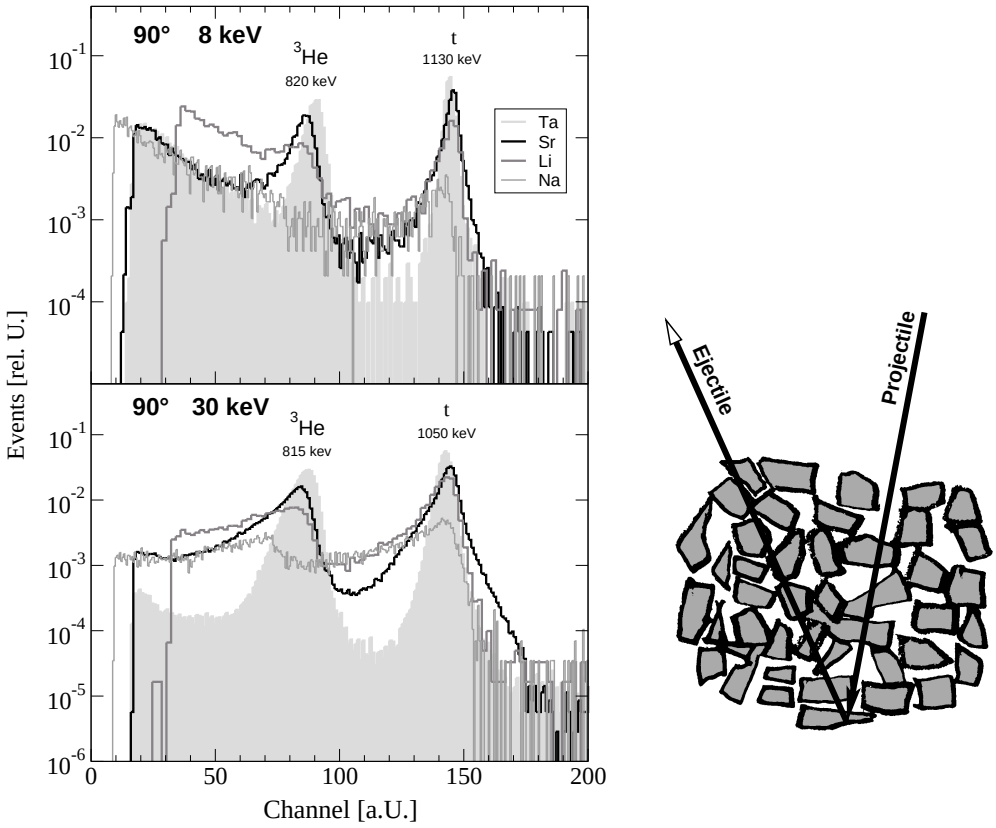

Figure 1: Normalized spectra from the 90°-detector. The low-energy tail complicates the discrimination and is caused by embrittlement which becomes stronger for more reactive metals. The sketch shows how different paths through the target explain the tails.

of the projectiles. The material dependence can be explained, too. Ta is almost a noble metal with low reactivity but nonetheless able to chemically bind hydrogen to high amounts. It just stretches its lattice dimensions but does not recrystallize like the highly reactive metals of the groups I and II of the periodic system. So there is no embrittlement and hardly a tail visible. On the other hand the effects of embrittlement and the tail increase from Sr over Li to Na with decreasing electron negativity. The symptoms were even visible, e.g. dust particles crumbled from a strontium target, the thickness of a natrium target grew considerably. The low-energy tail formation complicates the integration of the spectral lines till unfeasibility in the case of Na. The ^{3}He-line sits on the tail of the t-line. All efforts to describe and extrapolate the tail of the t-line to the lower energies analytically failed, since the form of the lines is dependent on the nucleus species, ejectile and projectile energy. Uncertainties and imponderabilities in the integral of the spectral lines are taken into account in the errors additionally to the counting statistic. Consequently they are the dominating error source. If in doubt, events were attributed to the ^{3}He-line only, gaining a conservative estimate at least. Fortunately, the tails are small at the low projectile

energies were the asymmetry in the branching ratios becomes observable.

Neglecting $l \geq 2$ contributions the angular distribution can be described as follows

$$\frac{d\sigma}{d\omega}(\vartheta) = A_0 + A_2 \cos^2 \vartheta \,. \tag{1}$$

Because of the identical bosons in the entrance channel the angular distribution is symmetric around 90°. ϑ and ω are the polar angle and the solid angle in the CM system, respectively. Since the experimentally determined thick target yield is dominated by the high energy contributions below the Coulomb barrier a similar expression is valid for the differential counting number

$$\frac{dN}{d\omega}(\vartheta) = a_0 + a_2 \cos^2 \vartheta \,. \tag{2}$$

The expansion coefficients a_0 and a_2 now include a constant factor containig a product of detector and target properties and the number of incident projectiles. A measurement at 20 keV for Sr exemplary shows the results for the differential counting number and the corresponding fitting function in fig. 2. The fit is computed with a non-iterative generalized linear fitting algorithm employing singular value decomposition thus allowing for more accurate values and better error handling. The data points obtained for the protons are included. As can be seen protons and tritons follow the same angular distribution. One observes a significantly stronger angular anisotropy for the neutron channel. The angular anisotropy is quantitatively given by the ratio $\frac{a_2}{a_0} = \frac{A_2}{A_0}$. Again with the previous argumentation the two fitting coefficients can be used to calculate the branching ratio of the two mirror reactions with

$$\frac{\sigma_{\mathrm{d(d,n)^3He}}}{\sigma_{\mathrm{d(d,p)t}}} = \frac{Y\left(^3\mathrm{He}\right)}{Y\left(\mathrm{p}\right)} = \frac{N\left(^3\mathrm{He}\right)}{N\left(\mathrm{p}\right)} = \frac{a_0\left(^3\mathrm{He}\right) + \frac{1}{3}a_2\left(^3\mathrm{He}\right)}{a_0\left(\mathrm{p}\right) + \frac{1}{3}a_2\left(\mathrm{p}\right)} \tag{3}$$

where in the last step N is simply the the integral over the unit sphere of the differential counting number (2). When calculating with the fitting coefficients one must consider that they are not independent variables. Then the Gaussian error propagation formula needs to be completed by a term containing the off-diagonal element of the covariance matrix from the fit. The results are plotted in fig. 3. The branching ratios and angular distributions determined for Ta, Al, Zr and Pd agree with the results of the gas target experiment [8]. Not so for Sr and Li. While for p there are no pecularities, for ^{3}He the anisotropy raises at lower energies (see also fig. 4). Simultaneously, the n branch is suppressed. The results for protons and tritons are concordant. The low quality of the Li points results from the ambiguity of the integration of the spectral lines with large low-energy tails. For the same reason, the spectra obtained for Na could not be analyzed quantitatively, though the spectra indicate a strong suppression of the neutron-proton ratio at low energies, too. For details refer to [4].

3 Theoretical considerations and discussion

The problems of integrating the overlapping spectral lines cannot be circumvented by the use of detector telescopes for particle identification. The ΔE-detector of the usual semiconductor detector telescopes would already absorb the recoil nuclei.

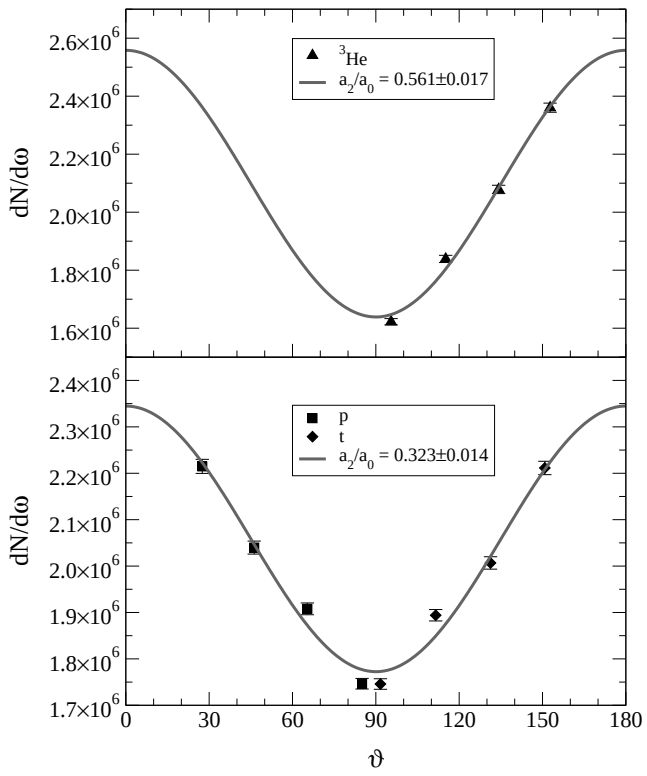

Figure 2: Angular distribution of the ^{2}H(d,p)^{3}H and ^{2}H(d,n)^{3}He reactions obtained at the deuteron energy $E_d = 20\,\mathrm{keV}$ for Sr.

The embrittlement cannot be responsible for the observed anomalous asymmetry in the branching ratios because the effects of embrittlement like tail formation rise with the projectile energy in contradiction to the deviations in the branching ratio. This is also valid for conceivable weird surface textures. Multiple scattering of the ejectiles in the thick target could possibly redirect leaving particles depending on the nucleus species and thereby change the detection rate. Such has been tested with a Monte Carlo simulation having given a negative result [9]. Furthermore anisotropic symmetries in crystal structures cause effects like optical activity and piezo and pyro electricity. So this could be a conceivable reason for the experimental observations. Enantiomorphy is a necessary condition for such effects. However, the point groups belonging to LiD, SrD_2 and NaD do not allow for this.

From the theoretical point of view the cross section for the mirror reactions ^{2}H(d,p)^{3}H and ^{2}H(d,n)^{3}He at deuteron energies below 100 keV can be described with 16 collision matrix elements, corresponding to S,P,D-waves in the entrance channel. The matrix elements for incoming D-waves cannot be omitted as frequently asserted since they are mandatory to describe the angular anisotropy down to the lowest energies. The values of the matrix elements are relatively

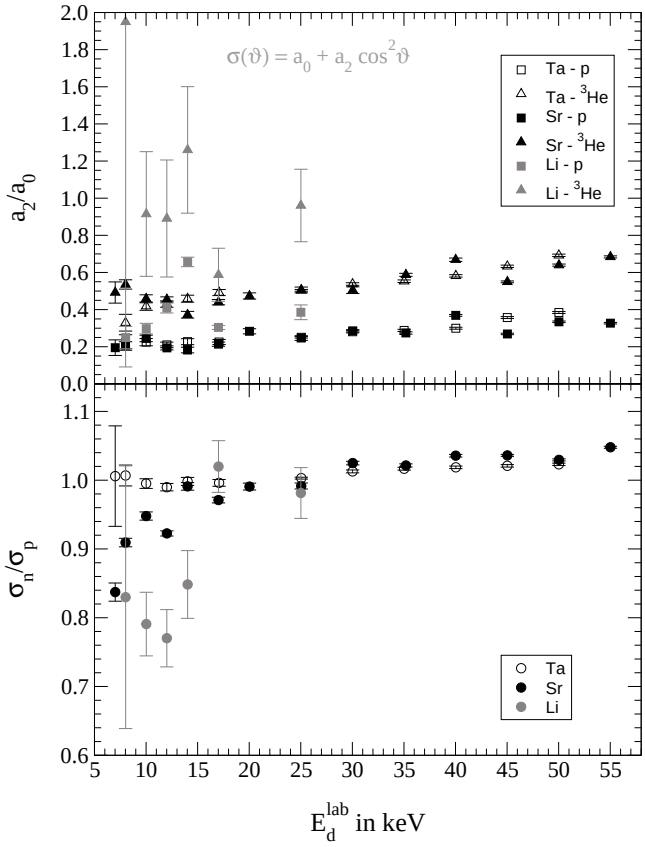

Figure 3: The upper part displays the anisotropy from the detection of the p and ^{3}He ejectiles. The lower part shows the branching ratio for the two mirror reactions.

well known and were obtained by fitting experimental cross sections, vector and tensor analyzing powers measured in gas target experiments [10, 11]. The differential cross section for both reactions can be presented by a coherent superposition of all sixteen matrix elements [5] (dashed line in fig. 4) and agrees with our results obtained for Al, Zr, Pd and Ta. In the case of Sr (also for Li) a polarization of the deuterons in the crystal lattice had to be assumed. A suppression of the channel spin $S = 0$ (spins of the deuterons are anti-parallel) and allowing the other channels with spins $S = 1, 2$ to be undisturbed permits to describe simultaneously the enhancement of the angular anisotropie of the ^{2}H(d,n)^{3}He reaction and the decrease of the n/p branching ratio at very low energies down to 0.83. The results of corresponding calculations are presented in fig. 4 as full lines. Here we have assumed that the deuteron polarization takes place gradually below the Fermi energy (for Sr about 25 keV), reaching its maximum value already below 10 keV. A strong quenching of the neutron channel might also be explained by different screening energies for relative angular momentum $L = 0, 1$. Supposing that the screening energy for the $L = 1$ contribution is much smaller than for $L = 0$ one gets a decreasing n/p branching ratio at low energies reaching a minimum of only 0.93. In this case, however, the anisotropy of the angular

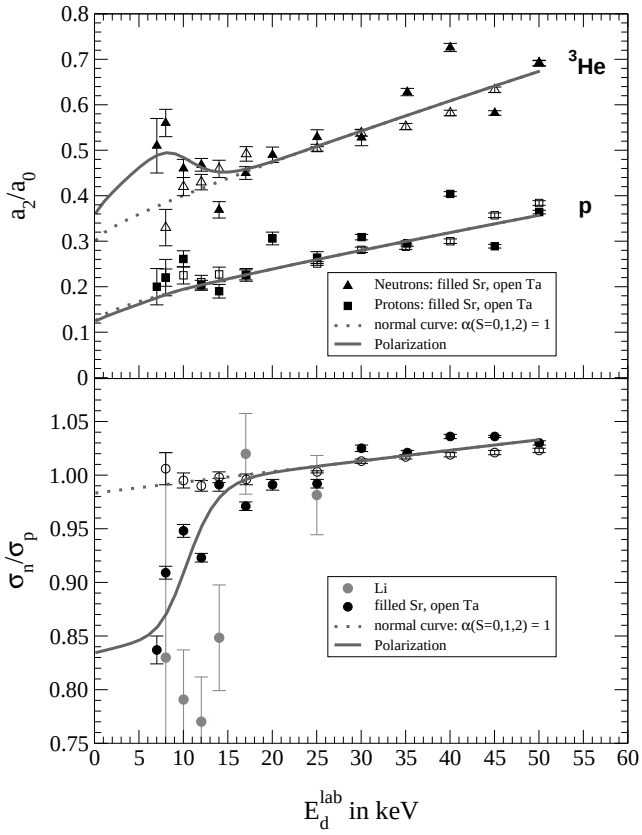

Figure 4: The dashed line represent the normal curve. The solid lines result from a deuteron polarization corresponding to a suppression of the $S = 0$ channel at lower energies.

distribution for both channels will be reduced till isotropy, in contradiction to the experimental results. For details refer to [5].

4 Conclusion

We presented a first experimental evidence for a alteration of the branching ratios in the d+d fusion reactions obtained in an accelerator experiment which can be theoretically explained by polarization of the reacting deuterons in the crystal lattice while other rather trivial causes could be excluded. The reason for the deuteron polarization is, however, still unknown. A distinctiveness of the (earth)alkaline metals is the formation of an ionic bond to hydrogen, which might be a starting point for a possible explanation based on the spin-spin interaction. In view of the experimental indications for a strong neutron-proton asymmetrie in the d+d reactions at room temperature, our experiment supports an understanding of the cold fusion phenomena although further efforts are necessary. An experiment with more sophisticated particle detection

techniques is in progress in order to refine the data.

References

[1] K. Czerski, A. Huke, P. Heide, M. Hoeft, and G. Ruprecht. In N. Prantzos and S. Harissopulos, editors, *Nuclei in the Cosmos V*, Proceedings of the International Symposium on Nuclear Astrophysics, page 152, Volos, Greece, July 6-11 1998. Editions Frontières.

[2] K. Czerski, A. Huke, A. Biller, P. Heide, M. Hoeft, and G. Ruprecht. *Europhys. Lett.*, 54(4):449–455, 2001.

[3] A. Biller, K. Czerski, P. Heide, M. Hoeft, A. Huke, and G. Ruprecht. In *Verhandlungen der DPG*, volume 1, page 28, Göttingen, 1997. DPG-Frühjahrstagung.

[4] A. Huke. *Die Deuteronen-Fusionsreaktionen in Metallen.* PhD thesis, Technische Universität Berlin, 2002.

[5] Tatiana Dorsch. Theoretische Untersuchung der anomalen Asymmetrie im Verzweigungsverhältnis der Reaktionen d(d,p)^{3}H und d(d,n)^{3}He im Verbund der Hydride der (Erd)Alkalimetalle. Diplomarbeit, Institut für Atomare Physik und Fachdidaktik der Technischen Universität Berlin, 2004.

[6] A. Huke, K. Czerski, and P. Heide. Accelerator experiments and theoretical models for the electron screening effect in metallic environments. Proceedings of the International Conference on Condensed Matter Nuclear Science, Marseille, France, November 2004. ICCF-11.

[7] William M. Mueller, James P. Blackledge, and George G. Libowitz, editors. *Metal Hydrides.* Academic Press, New York, London, 1968.

[8] Ronald E. Brown and Nelson Jarmie. *Phys. Rev. C*, 41(4):1391, 1990.

[9] Alexander Biller. Einfluß der Vielfachstreuung auf Dicktarget-Yields in niederenergetischen Kernreaktionen. Diplomarbeit, Institut für Atomare und Analytische Physik der Technischen Universität Berlin, 1998.

[10] H. Paetz gen. Schieck and S. Lemaitre. *Ann. Phys.*, 2:503, 1993.

[11] O. Geiger, S. Lemaître, and H. Paetz gen. Schick. *Nucl. Phys.*, A(586):140–150, 1995.